Angewandte Chemie
Eine Zeitschrift der Gesellschaft Deutscher Chemiker

Supporting Information

NH_4^+ Deprotonation at Interfaces Induced Reversible H_3O^+/NH_4^+ Co-insertion/Extraction

M. Huang, Q. He, J. Wang, X. Liu, F. Xiong, Y. Liu, R. Guo, Y. Zhao, J. Yang*, L. Mai**

Supporting Information

NH_4^+ Deprotonation at Interfaces Induced Reversible H_3O^+/NH_4^+ Co-insertion/Extraction

Meng Huang,[+,a,b] Qiu He,[+,c] Junjun Wang,[b] Xiong Liu,[e] Fangyu Xiong,[b,f] Yu Liu,[b,g] Ruiting Guo,[b] Yan Zhao,*[c,d] Jinlong Yang,*[a] Liqiang Mai0000-0003-4259-7725*[b]

[a] Guangdong Research Center for Interfacial Engineering of Functional Materials, College of Materials Science and Engineering, Shenzhen University
Shenzhen, 518060, China
E-mail: yangjl18@szu.edu.cn

College of Physics and Optoelectronic Engineering, Shenzhen University
Shenzhen, 518060, China

[b] State Key Laboratory of Advanced Technology for Materials Synthesis and Processing, Wuhan University of Technology
Wuhan, 430070, China
E-mail: mlq518@whut.edu.cn

[c] College of Materials Science and Engineering, Sichuan University
Chengdu, 610065, China
E-mail: yan2000@whut.edu.cn

[d] The Institute of Technological Sciences, Wuhan University
Hubei, Wuhan 430072, China

[e] School of Materials Science and Engineering, Zhengzhou University
Zhengzhou, 450001, China

[f] Department of Physics, City University of Hong Kong
Tat Chee Avenue, Kowloon, 999077, Hong Kong, China

[g] Department of Materials Science and Engineering, National University of Singapore
Singapore, 117574, Singapore

[+] These authors contributed equally to this work.

Experimental Section

Synthetic procedures for VO_2(B): The typical synthesis process of VO_2(B) is described as follows: 600 mg V_2O_5 (AR, purchased from Sinopharm Chemical Reagent Co., Ltd) was added into 80 mL mixed solution (60 ml deionized water and 20 ml ethylene glycol). After stirring for 45 min under room temperature, the resulting suspension was transferred to an 80 ml autoclave then heated at 180 °C for 9 h. After complete reaction, the obtained precipitates were collected by centrifugation and washed with water and pure ethanol for 3 times, respectively. The washed solid products were dried at 70 °C for over 12 h.

Synthetic procedures for $(NH_4)_2CuFe(CN)_6$: The typical synthesis process of $(NH_4)_2CuFe(CN)_6$ is described as follows: Add 50 mL solution containing 3.0 mmol $CuSO_4$•$5H_2O$ (AR, purchased from Sinopharm Chemical Reagent Co., Ltd) into 100 mL solution dissolving 0.2 g ascorbic acid, 2.0 mmol $K_4Fe(CN)_6$•H_2O (AR, purchased from Sinopharm Chemical Reagent Co., Ltd) and 2.0 g $(NH_4)_2SO_4$ (GR, purchased from Sinopharm Chemical Reagent Co., Ltd) drop by drop under stirring at 60 °C for 2 h. After complete reaction, the obtained solution was aged for several hours until the precipitates were collected by centrifugation and washed with water and pure ethanol for 3 times, respectively. The washed solid products were dried at 70 °C for over 12 h.

Characterization: The morphology was observed by using the field emission scanning electron microscopy (SEM, JEOL JSM-7100F, acceleration voltage: 15 kV). Transmission electron microscope (TEM), and high-resolution TEM (HRTEM) images were collected by using a CEOS probe corrected FEI Themis TEM with 300 kV accelerating voltage. The BET surface area was calculated from nitrogen adsorption isotherms collected at 77 K using a Tristar-3020 instrument. XPS measurements were carried out using an VG MultiLab 2000 instrument. The powder X-ray diffraction (XRD) were collected on a D8 Advance X-ray diffractometer using Cu Kα radiation (λ = 1.5418 Å). *In situ* XRD experiments were performed using Bruker D8 Discover X-ray diffractometer with a nonmonochromated Cu Kα X-ray source (Power = 1600

W, λ = 1.5418 Å). For *in-situ* XRD measurements, the positive electrode was covered by a titanium foil with a small hole which was covered with polyethylene plastic wrap. The signals were received by the planar detector in a still mode during the testing process. The VO_2(B) electrodes were fresh, and each pattern took 100 s to acquire at the discharge/charge current density of 150/250 mA g^{-1}. *In-situ* ATR-FTIR measurements using a Thermo scientific iS50 spectrometer. A ZnSe prism beveled at 60° constituted the bottom of the electrochemical cell. The spectra were collected in external reflection using a liquid-N2-cooled MCT (mercury−cadmium−telluride) detector. The single-beam spectra were acquired at 4 cm^{-1} spectral resolution with an interferometer frequency of 40 kHz and then Fourier transformed. Each pattern was acquired at each 60 s at the discharge/charge current density of 150/250 mA g^{-1}. TGA was performed on an STA-449C thermobalance in air atmosphere with a temperature ramp of 10 °C min^{-1}.

Calculation method

A series of calculations based on density functional theory were completed using Vienna Ab initio Simulation Package (VASP)[1]. The embedding of different particles (H^+, Li^+, Na^+, K^+, $NH4^+$-H^+) into the internal hollow space of VO_2 bulks and the adsorption onto VO_2 (100) surfaces were simulated. For all calculations, Perdew-Burke-Ernzerhof exchange-correlation functional[2] were used with spin polarization. The plan-wave cutoff energy of 520 eV for the projector augmented wave (PAW) method[3] and Gamma point centered k-mesh in Brillouin zone with separation of 0.04×2π $Å^{-1}$ were set. The Grimme-D3 method[4] was applied to correct the dispersion force and the Climbing Image Nudged Elastic Band (CI-NEB) method[5] was used to simulate the migration of different particles. The energy difference should be lower than 10^{-5} eV $atom^{-1}$ to reach electronic self-consistent field convergence, and the force should be lower than 0.02 eV $Å^{-1}$ to reach the convergence for ionic step in geometric optimizations. The cell lattices of VO_2 bulks were relaxed when embedded with particles, and a half of atoms at the bottom of VO_2 (100) slabs were fixed for

surface simulation. The VO_2 bulks contains 64 O and 32 V atoms, and a unit VO_2 (100) surface contains 16 O and 8 V atoms. The Gibbs free energies of the hydrolysis reaction of NH_4^+ and H_2O in water environment at 298.15 K were calculated by Dmol3 module implemented in Materials Studio software with M06-L density functional.[6] The calculation quality was set as fine and the basis set of double Numerical plus polarization was applied.

Electrochemical tests: The concentration of Li-E, Na-E and K-E is 1.5, 3.0 and 3.0 M, respectively. H-E and NH-E were prepared by dissolving 1 g CH_3COOH and CH_3COONH_4 in 6 g deionized water, respectively. Hy-E was prepaerd by adding 1 g CH_3COOH in 35 g NH-E. EG-E was prepared by dissolving 1 g CH_3COONH_4 in 6 g ethylene glycol.

The electrode paste films were prepared by mixing active materials, ketjen black, and polytetrafluoroethylene (7:2:1). Then, the paste films were dried for at least 12 h at 70 °C and pressed onto the Ti mesh. The mass loading of active materials was ~8 mg cm^{-2}. The cyclic voltammetry (CV) and the galvanostatic charge/discharge tests of the individual electrode sample were carried out in three-electrode setup (paste film on Ti mesh as the working electrode, SCE as reference electrode and Pt plate as counter-electrode) in different electrolytes using an electrochemical workstation (CHI 760E/605E). The assembled VO_2(B)//($(NH_4)_2CuFe(CN)_6$) 2032 coin cells were at the mass ratio of active materials of ~6.7($(NH_4)_2CuFe(CN)_6$) :1(VO_2(B)). The assembled VO_2(B)//($(NH_4)_2CuFe(CN)_6$) pouch cells were at the mass ratio of active materials of ~6($(NH_4)_2CuFe(CN)_6$) :1(VO_2(B)).The Whatman glass microfiber filter (Grade GF/A) was used as the separator. And the galvanostatic charge/discharge tests of the coin cells were performed using a Battery Testing System (CT-ZWJ-4'S-T-1U) from Neware Technology Co.,Ltd., Shenzhen, China.

Table S1. Crystallographic data and powder XRD Rietveld refinement results for VO_2(B): atomic coordinates, site occupancies, isotropic displacement parameters and

reliability factors at room temperature.

Crystal System			**Monoclinic**			
Space Group			*C 2/m*			
Lattice Parameter			a=12.0536(0) Å, b=3.6938(8) Å, c=6.4217(3) Å α = γ = 90.00°, and β = 106.9247°			
Atoms	x	y	z	Wyckoff	Occupancy	Uiso
V1	0.30033	0.50000	0.71470	4i	1.000	0.023
V2	0.39750	0.50000	0.31507	4i	1.000	0.017
O1	0.36373	0.50000	0.98612	4i	1.000	0.117
O2	0.23621	0.50000	0.33288	4i	1.000	0.018
O3	0.46054	0.50000	0.65890	4i	1.000	0.089
O4	0.12172	0.50000	0.67597	4i	1.000	0.001

* Rwp =5.58%, Rp =4.10%, χ^2 = 6.436

Table S2. Insertion energy and ionic radius of H^+, Li^+, Na^+, K^+, and NH_4^+ and their hydrated states.

Ion	**Insertion energy (eV)**		**Radius (Å)[7]**	
	Solo Ion	**Hydrated Ion**	**Cation Radius**	**Hydrated Radius**
Li^+	−2.10	−2.97	0.6	3.82
Na^+	−2.78	−2.48	0.95	3.58
K^+	−2.21	−2.44	1.33	3.31
NH_4^+	−2.53	−1.73	1.48	3.31
H_3O^+	−2.30	−2.56	1.0	2.82

Table S3. The ionic conductivity of different electrolytes, measured by conductivity meter (DDS-307A) at room temperature.

Electrolyte	**Conductivity**
Li-E	79.2 mS cm^{-1}

Na-E	88.8 mS cm^{-1}
K-E	122.1 mS cm^{-1}
NH-E	102.8 mS cm^{-1}
Hy-E	98.1 mS cm^{-1}
H-E	1663 μS cm^{-1}
Deionized water	1.0 μS cm^{-1}

Table S4. The pH values of different electrolytes at room temperature.

Electrolyte	**pH value**
Li-E	9.29
Na-E	9.75
K-E	6.12
NH-E	7.07
Hy-E	5.46
H-E	2.21

Table S5. Atomic ratio in as-prepared $(NH_4)_2CuFe(CN)_6$ collected by XPS spectrum.

Element	Atomic Frac.
C	46.5%
O	5.7%
Fe	7.1%
Cu	6.3%
K	0.4%
N	34.0%

Table S6. Crystallographic data and powder XRD Rietveld refinement results for $(NH_4)_2CuFe(CN)_6$: atomic coordinates, site occupancies, isotropic displacement parameters and reliability factors at room temperature.

Crystal System	**Cubic**
Space Group	*F - 4 3 m*

Lattice Parameter	A = b = c =10.0523(1) Å α = γ = β = 90.00°					
Atoms	x	y	z	Wyckoff	Occupancy	Uiso
Cu1	0.50000	0.50000	0.50000	4b	1.000	0.053
Fe1	0.00000	0.00000	0.00000	4a	1.000	0.054
C1	0.20010	0.00000	0.00000	24f	1.000	0.317
N1	0.30535	0.00000	0.00000	24f	1.000	0.062
N2	0.25000	0.25000	0.25000	4c	0.878	0.063
N3	0.75000	0.75000	0.75000	4d	0.938	0.066
K1	0.25000	0.25000	0.25000	4c	0.122	0.063
K2	0.75000	0.75000	0.75000	4d	0.062	0.066

* Rwp =1.48%, Rp =1.06%, χ^2 = 2.571

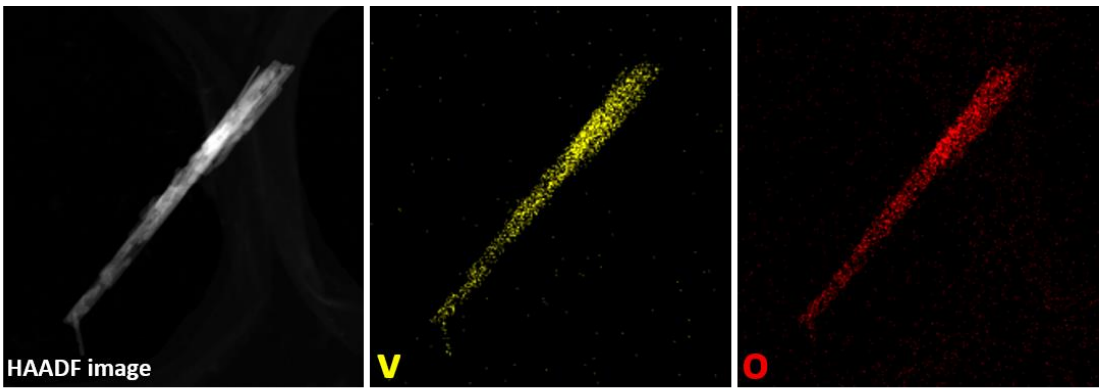

Figure S1. Energy-dispersive X-ray spectra of the as-prepared VO_2(B).

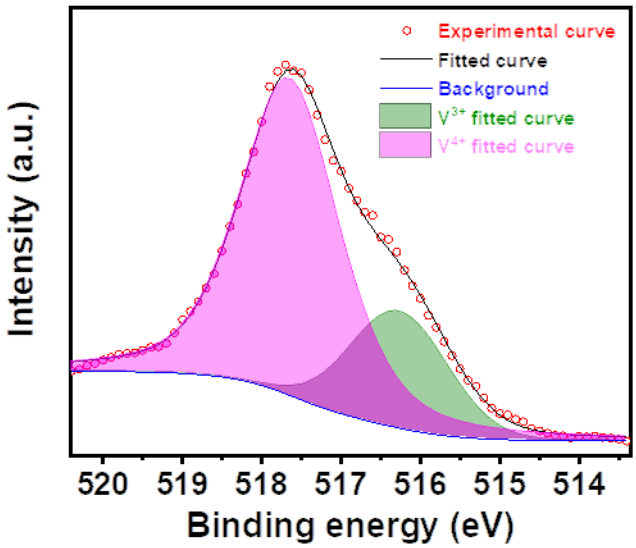

Figure S2. XPS spectrum of V 2p of the fresh electrode paste film.

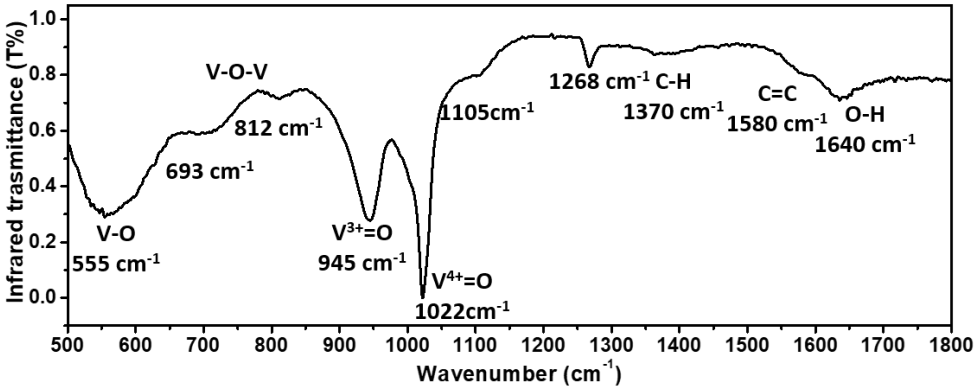

Figure S3. IR spectrum of as-prepared VO_2(B) powder. ***Dear editor, we have revised "V^{4+}=O" and "V^{5+}=O" to "V^{3+}=O" and "V^{4+}=O", respectively in Figure S3.***

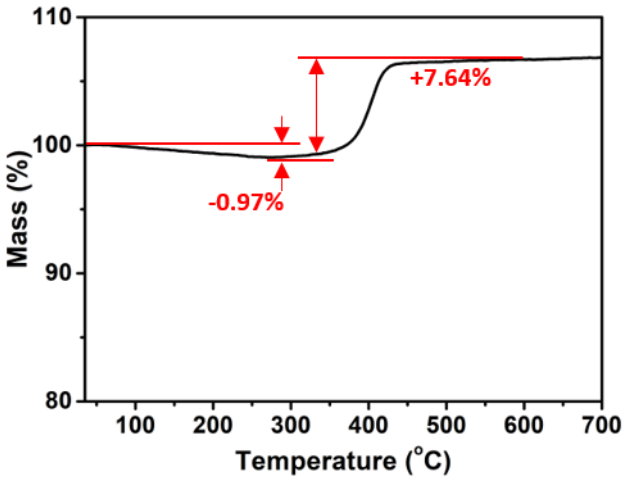

Figure S4. TGA profile of as-prepared VO_2(B) powder.

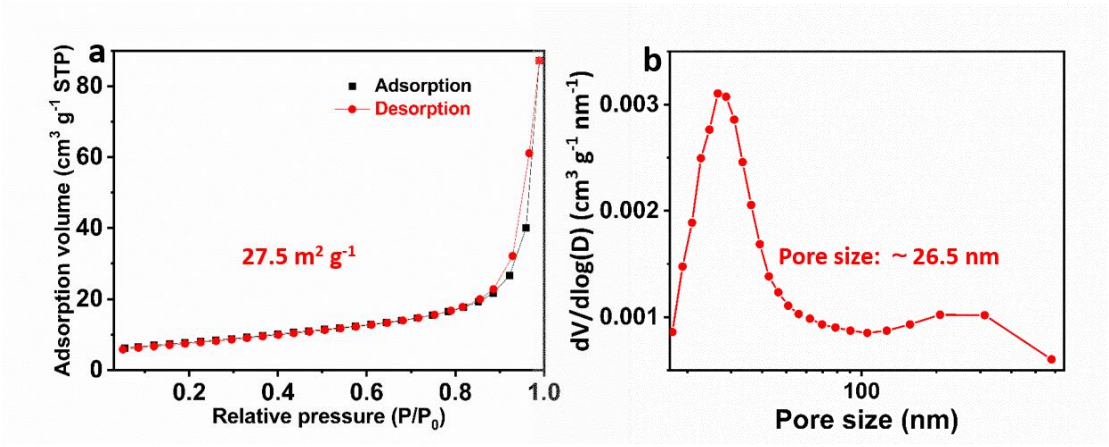

Figure S5. (a) The nitrogen adsorption–desorption isotherm curve. (b) The corresponding pore size distribution.

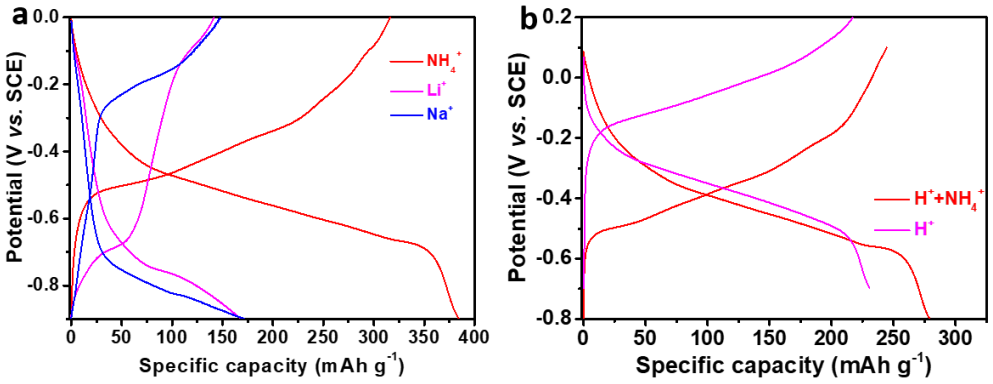

Figure S6. Charge/discharge profile of VO_2(B) electrode in different electrolytes at the current density of 500 mA g^{-1}.

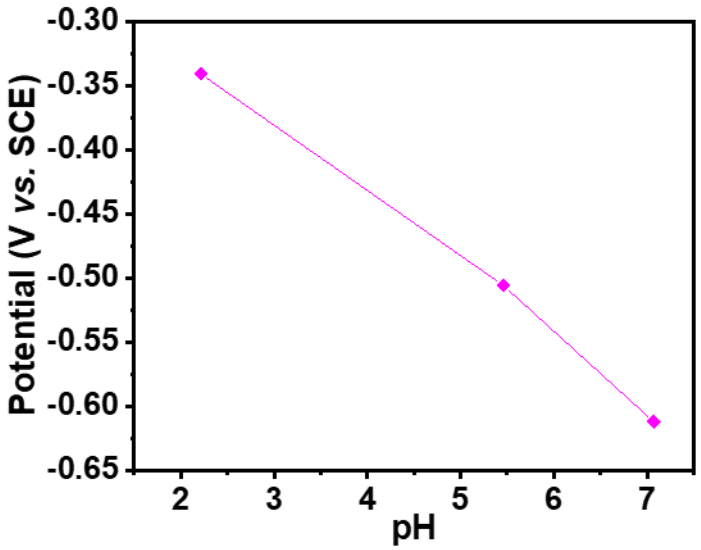

Figure S7. Equilibrium potential as a function of pH (different electrolyte).

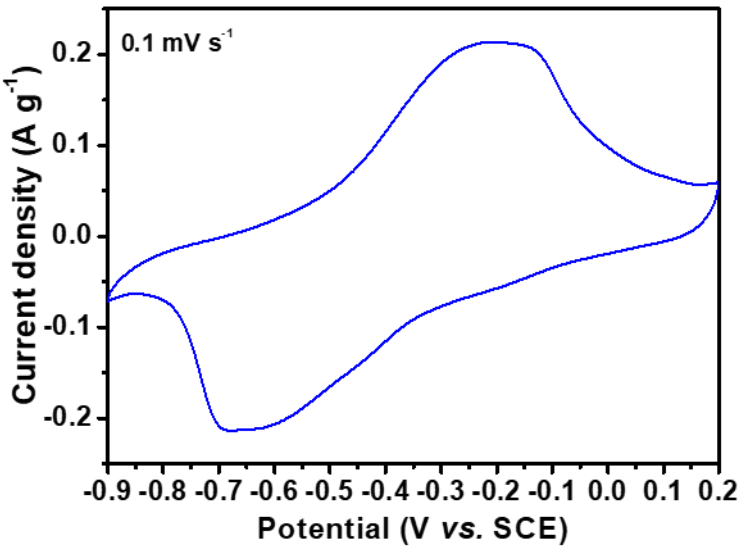

Figure S8. CV curves of VO_2(B) in EG-E electrolyte.

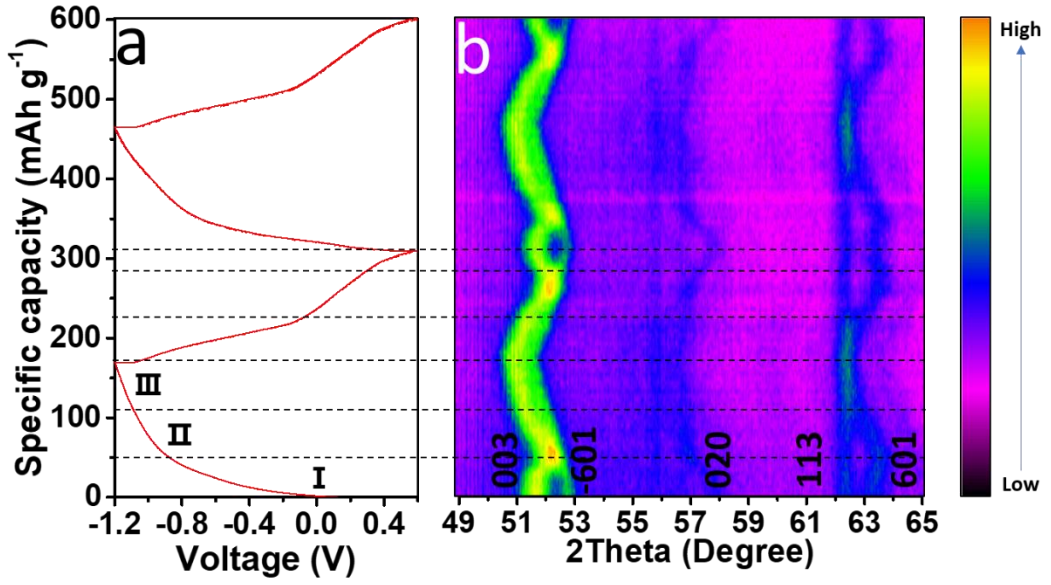

Figure S9. *In-situ* XRD characterizations of VO_2(B) materials in 3 M $NaClO_4$ electrolytes. (a) Charge/discharge profiles at a current density of 150 mA g^{-1}; (b) corresponding 2D XRD patterns using Bruker D8 Discover X-ray diffractometer with a nonmonochromated Co Kα X-ray source (λ = 1.7902 Å).

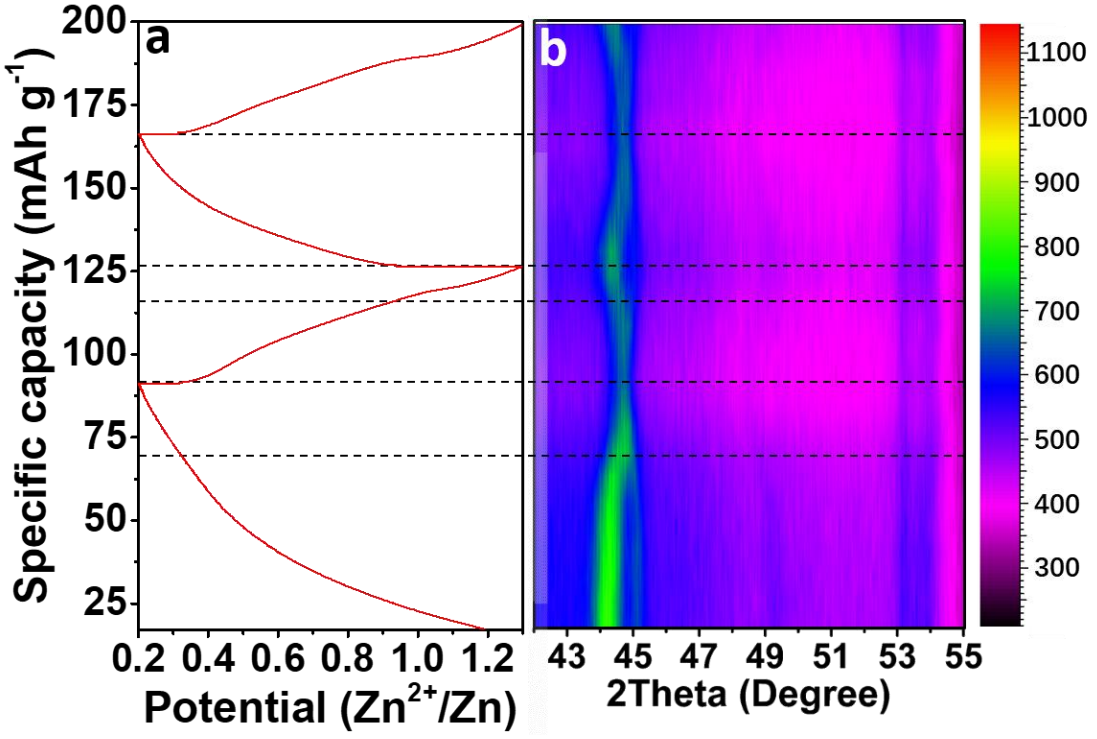

Figure S10. *In-situ* XRD characterizations of VO_2(B) materials in 3 M KCF_3SO_3 electrolytes. (a) Charge/discharge profiles at a current density of 150 mA g^{-1}; (b) corresponding 2D XRD patterns using Bruker D8 Discover X-ray diffractometer with a nonmonochromated Cu Kα X-ray source (Power = 1600 W, λ = 1.5418 Å).

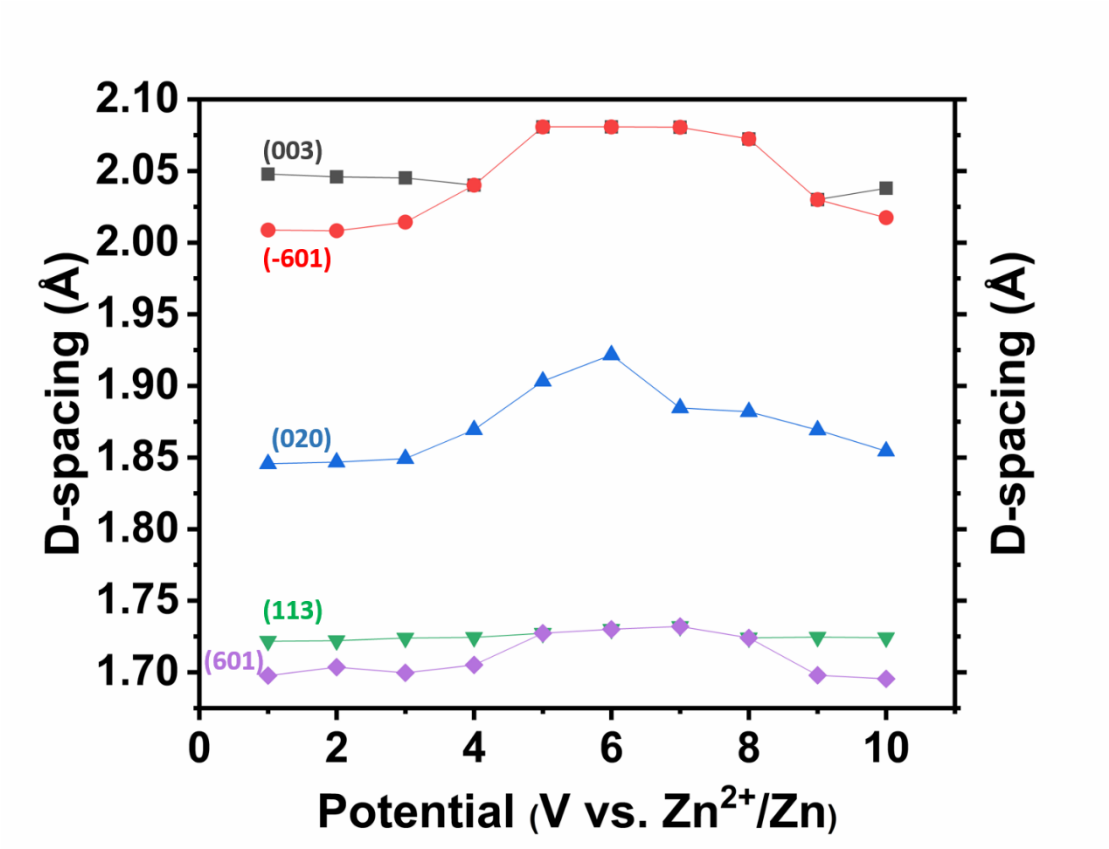

Figure S11. Lattice spacing of different planes at various discharge/charge state.

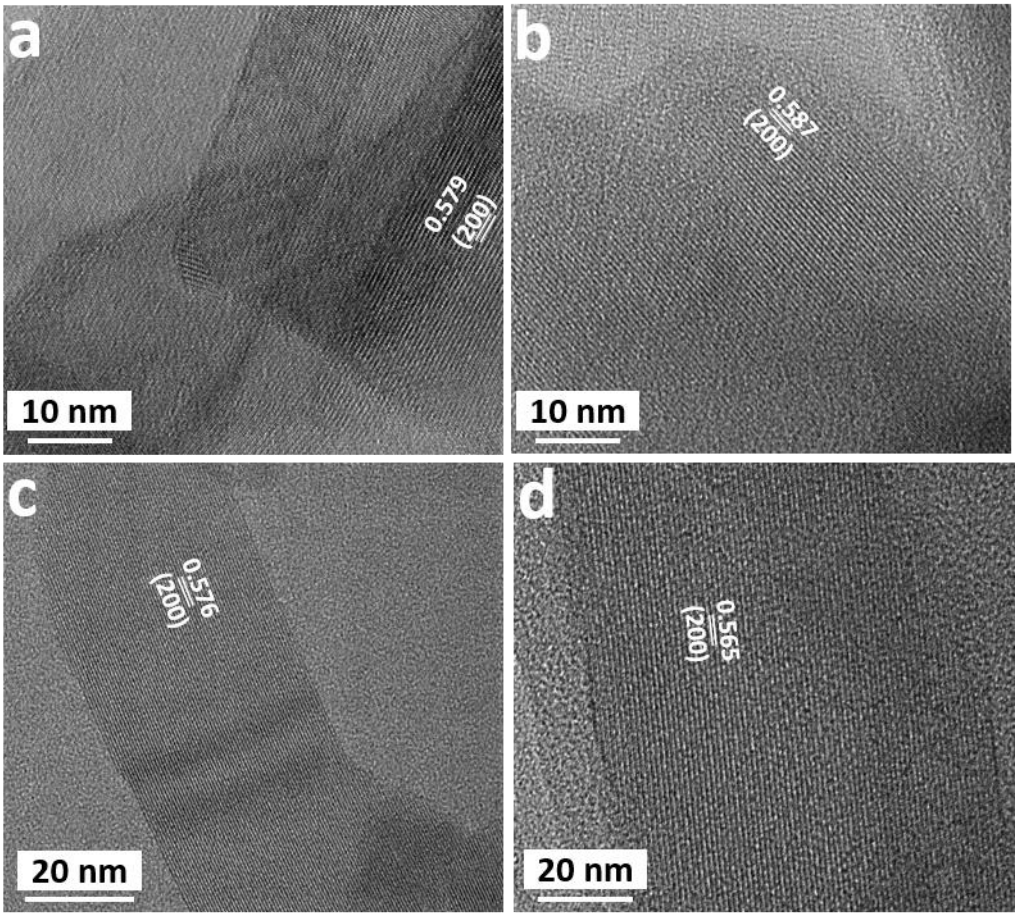

Figure S12. HRTEM images of VO_2(B) at different discharge/charge states: (a) discharged state at –0.5 V, (b) discharged state at –0.9 V, (c) charged state at –0.5 V, (d) charged state at –0.0 V.

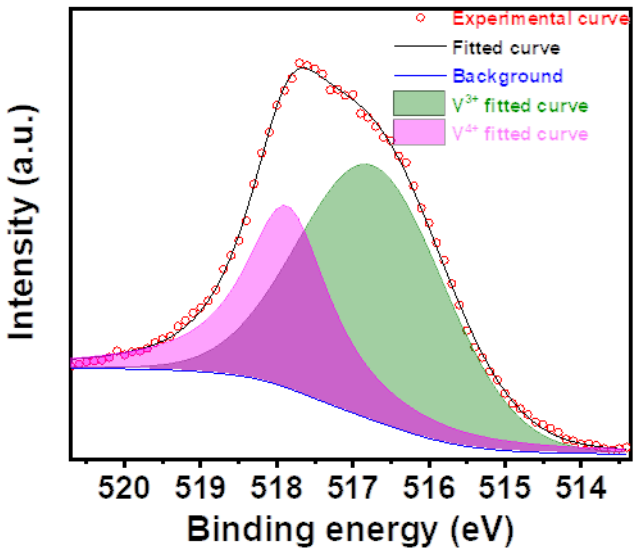

Figure S13. V 2p XPS fits of VO_2(B) at discharged state of −0.9 V.

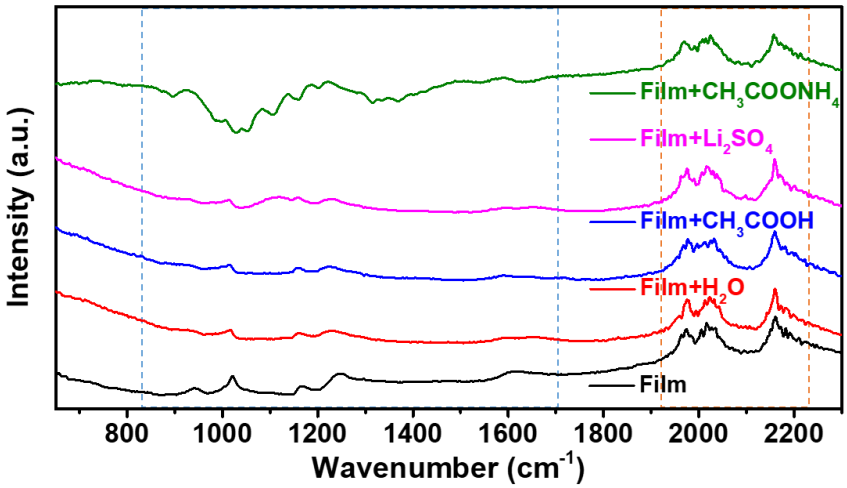

Figure S14. ATR-FTIR spectra of fresh VO_2(B) electrode films after soaked in different electrolytes.

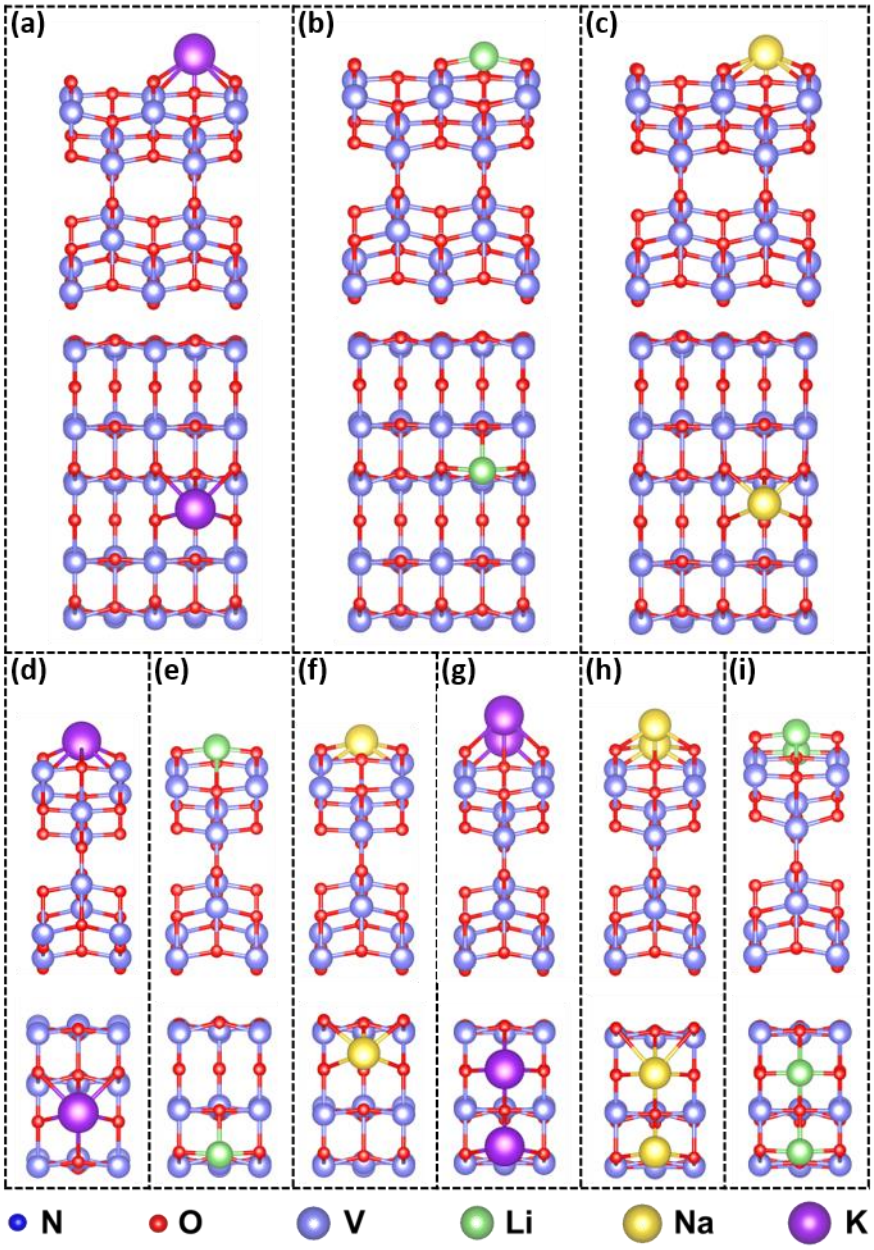

Figure S15. Optimized adsorption structures of Li^+, Na^+ and K^+ on VO_2(B) surface with different coverage rates: (a-c) one cation on a 2×2 supercell, (d-f) one cation on a 1×1 supercell, (g-i) two cations on a 1×1 supercell.

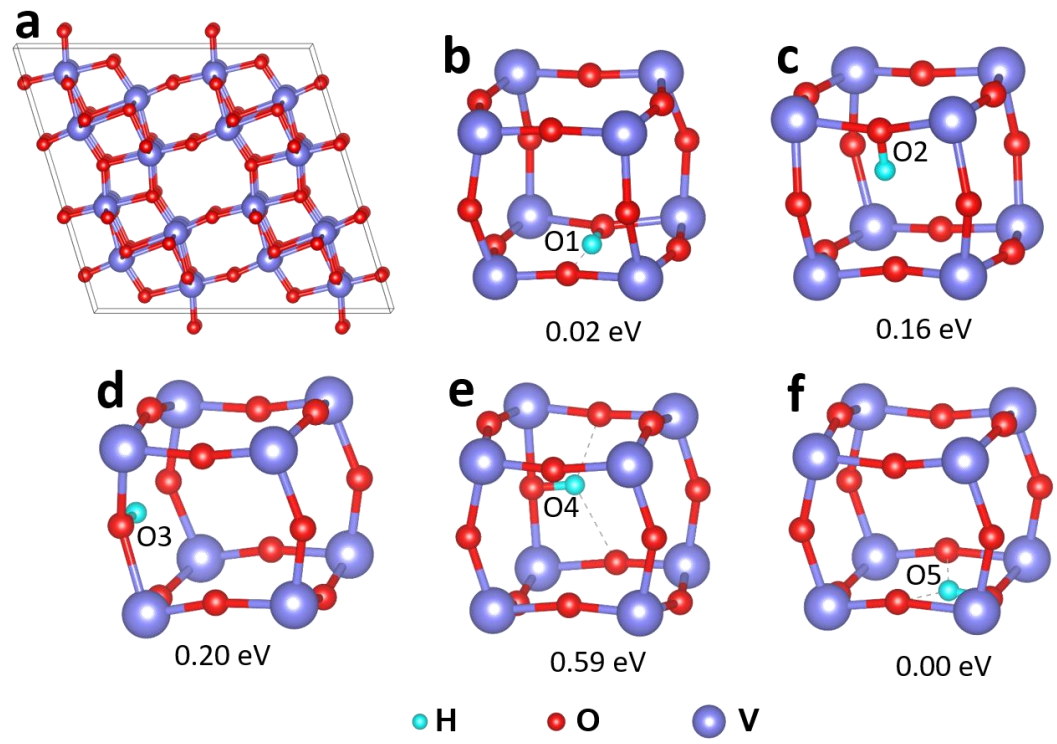

Figure S16. Different storage sites for H^+ with relative energy.

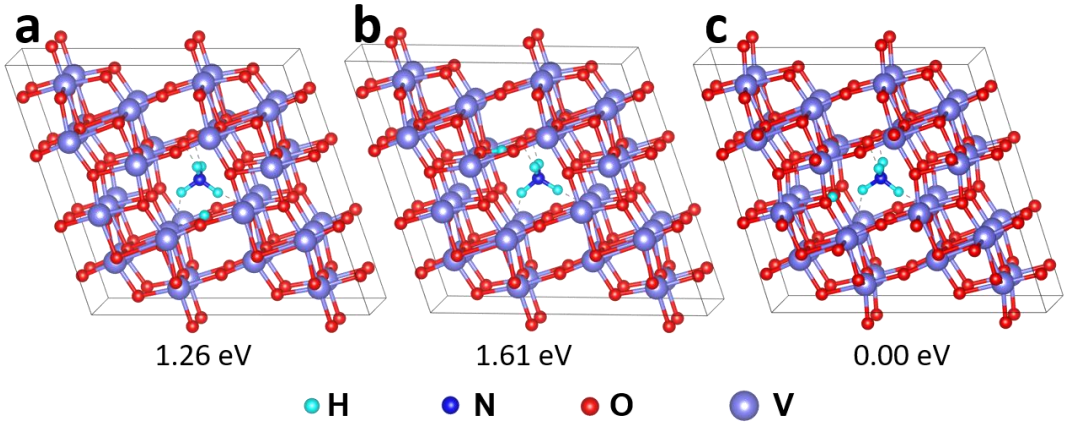

Figure S17. Different storage sites for H^+ and NH_4^+ with relative energy.

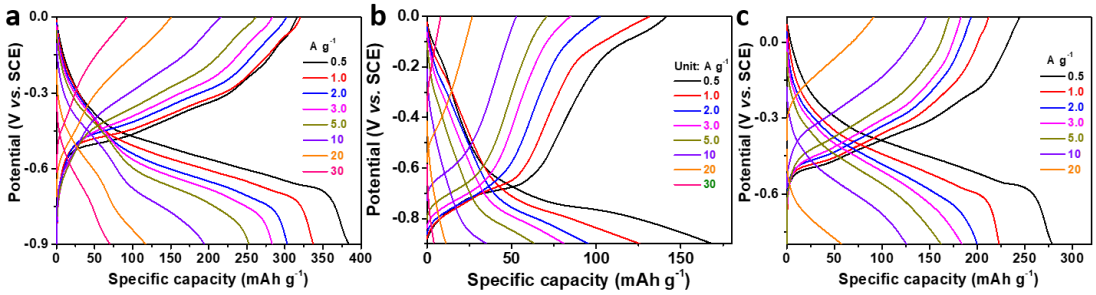

Figure S18. Discharge/charge profiles at current densities in the arrangement of 0.5 to 30 A g^{-1} in (a) NH-E, (b) Li-E, and (c) Hy-E.

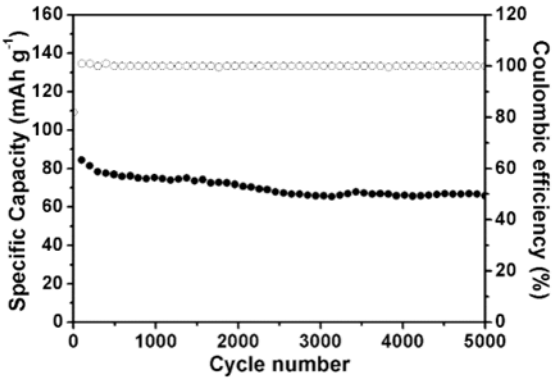

Figure S19. Cycling performance of VO_2(B) electrode materials in CH_3COONH_4 electrolyte at a current density of 20 A g^{-1}.

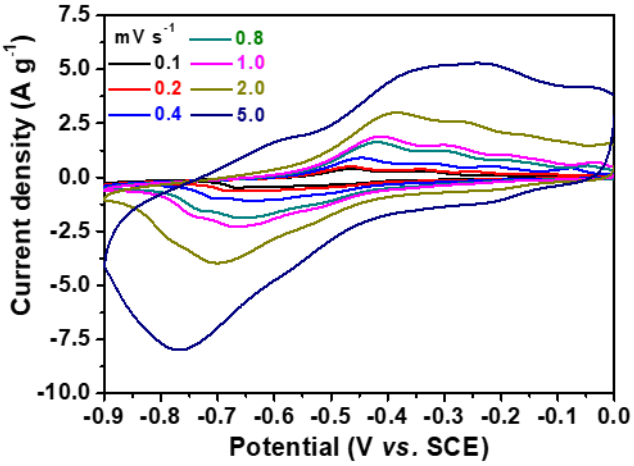

Figure S20. CV curves of VO_2(B) electrodes in NH-E at different scan rates from 0.1 to 5.0 mV s^{-1}.

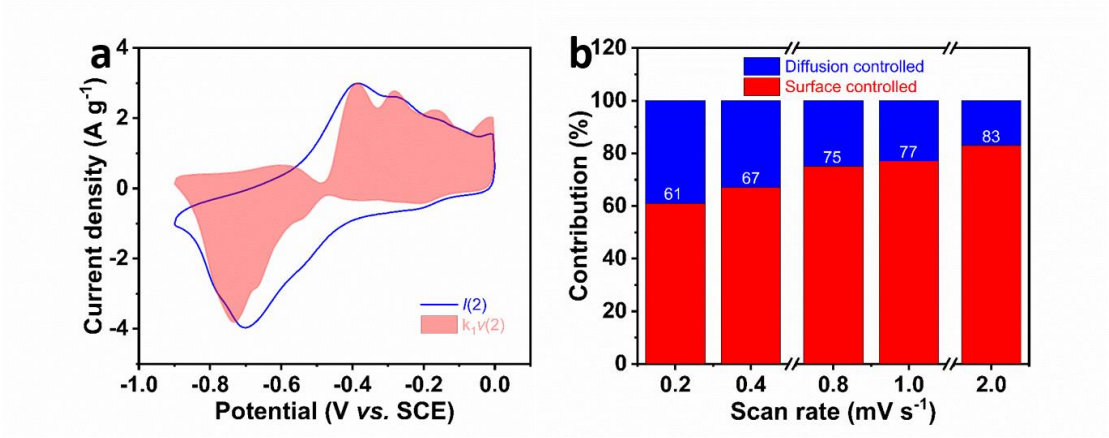

Figure S21. (a) Capacitive contribution (sky blue part) and diffusion contribution (void part) at 0.1 mV s^{-1}. (b) Normalized capacitive (red part) and diffusion-controlled (blue part) contribution ratios from 0.2 to 2.0 mV s^{-1}.

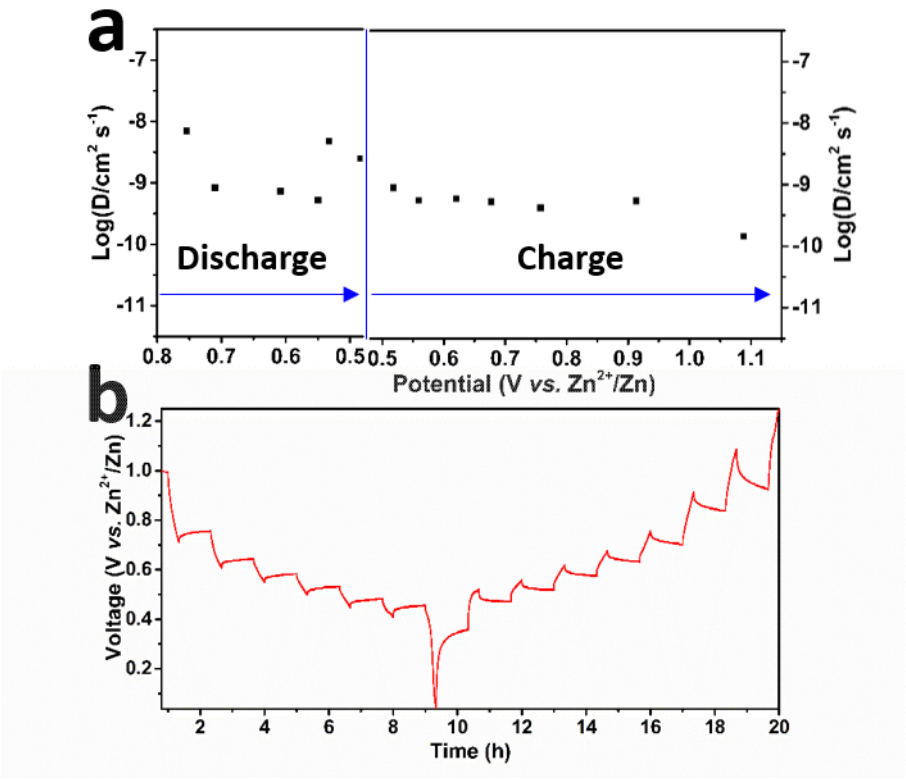

Figure S22. The GITT curves of VO_2(B) electrode. (a) ion diffusivity versus the state of discharge/charge. (b) GITT potential response curve with time. The experiment was conducted at constant current pulse of 150 mA g^{-1} for 20 min followed by a relaxation period of 60 min.

$$D = \frac{4}{\pi\tau}\left(\frac{m_B V_M}{M_B S}\right)^2 \left(\frac{\triangle E_S}{\triangle E_\tau}\right)^2$$

Scheme 1. Where τ refers to constant current pulse time, m_B, V_M, M_B, and S are the mass, molar volume, molar mass of the cathode material, and electrode-electrolyte interface area, respectively. $\triangle E_S$ is voltage difference during a single-step experiment, and $\triangle E_\tau$ is the total change of cell voltage during a constant current pulse excluding the IR drop.

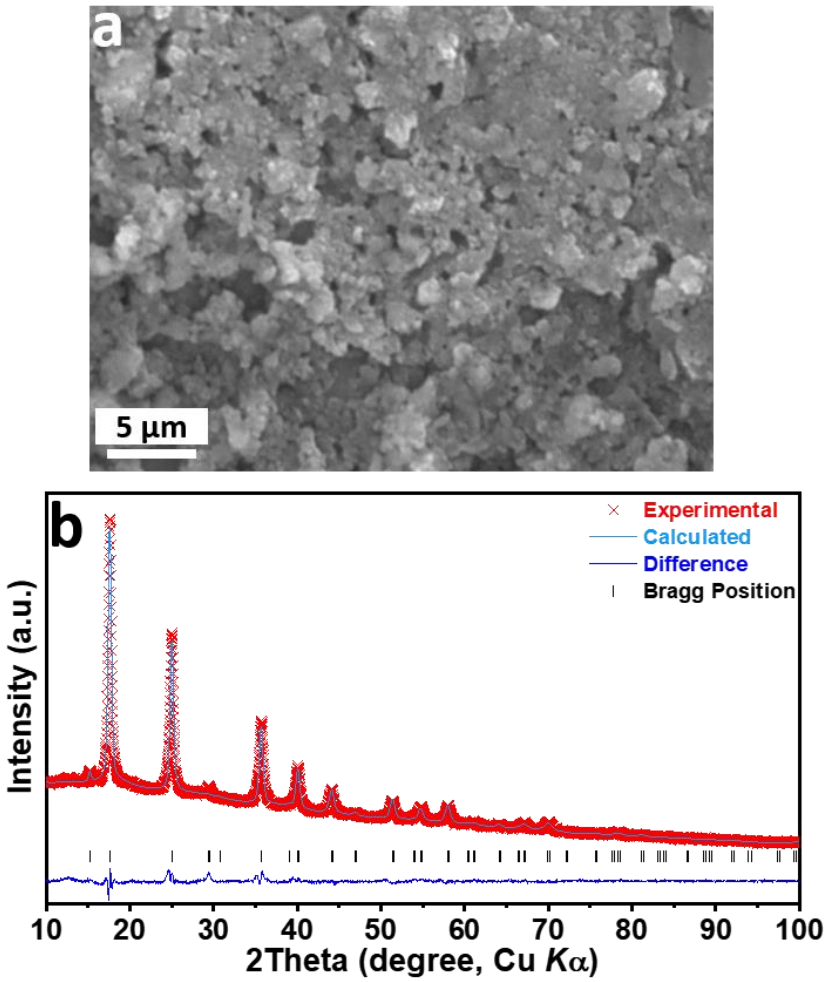

Figure S23. (a) SEM image and (b) XRD pattern of $(NH_4)_2CuFe(CN)_6$ powder.

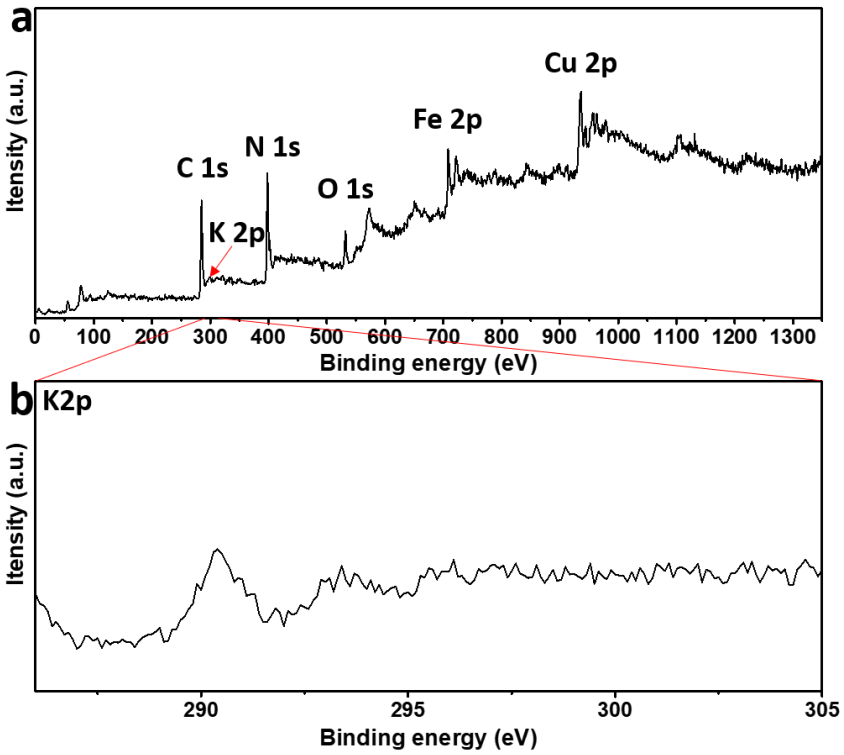

Figure S24. XPS spectra of $(NH_4)_2CuFe(CN)_6$ powder.

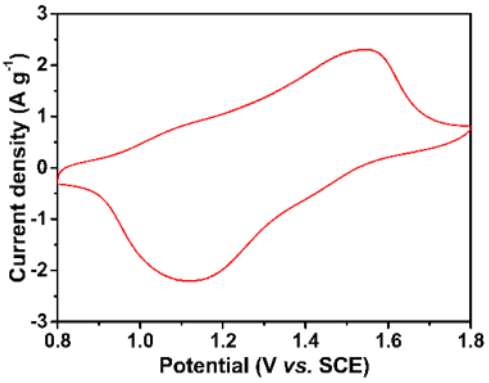

Figure S25. CV curve of $VO_2(B)//(NH_4)_2CuFe(CN)_6$ full battery at 2.0 mV s^{-1}.

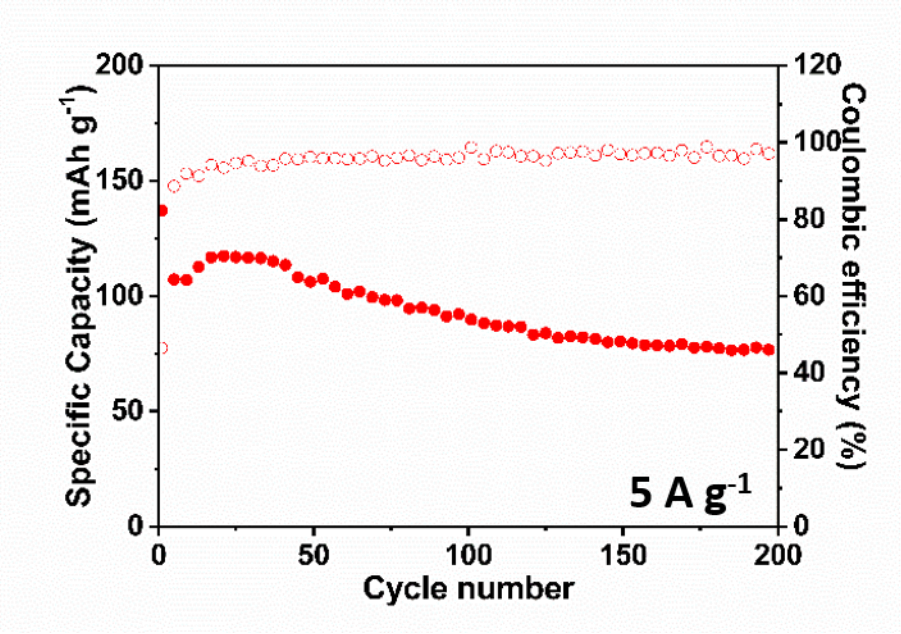

Figure S26. Cycling performance of VO_2(B)//$(NH_4)_2CuFe(CN)_6$ full battery at a current density of 5 A g^{-1}.

Reference

[1] G. Kresse, J. Furthmüller, *Phys. Rev. B* **1996**, *54*, 11169–11186.
[2] J. P. Perdew, K. Burke, M. Ernzerhof, *Phys. Rev. Lett.* **1996**, *77*, 3865–3868.
[3] G. Kresse, D. Joubert, *Phys. Rev. B* **1999**, *59*, 1758–1775.
[4] S. Grimme, J. Antony, S. Ehrlich, H. Krieg, *J. Chem. Phys.* **2010**, *132*, 154104.
[5] G. Henkelman, B. P. Uberuaga, H. Jónsson, *J. Chem. Phys.* **2000**, *113*, 9901–9904.
[6] a) B. Delley, *J. Chem. Phys.* **2000**, *113*, 7756-7764; b) Y. Zhao, D. G. Truhlar, *Theor. Chem. Acc.* **2008**, *120*, 215-241.
[7] D. Chao, H. J. Fan, *Chem.* **2019**, *5*, 1359-1361.